Lepton pair production in ultraperipheral collisions: Toward a precision test of the resummation formalism

Ding Yu Shao,[1,2] Cheng Zhang,[1] Jian Zhou,[3] and Ya-jin Zhou[3]

[1]*Department of Physics, Center for Field Theory and Particle Physics, Key Laboratory of Nuclear Physics and Ion-beam Application (MOE), Fudan University, Shanghai 200433, China*
[2]*Shanghai Research Center for Theoretical Nuclear Physics, NSFC and Fudan University, Shanghai 200438, China*
[3]*Key Laboratory of Particle Physics and Particle Irradiation (MOE), Institute of Frontier and Interdisciplinary Science, Shandong University, QingDao, China*

(Received 16 August 2023; accepted 21 November 2023; published 18 December 2023)

We present a detailed investigation of the azimuthal asymmetries and acoplanarity in lepton pair production in ultraperipheral collisions (UPCs). These observables provide a unique opportunity to test the soft colliner effective theory resummation formalism, given the exceptionally high photon flux in UPCs, which enables precise measurements of these processes. We improve the accuracy of the previous calculations by including the soft photon contributions beyond the double leading logarithm approximation. Notably, the single logarithmic terms arising from the collinear region are greatly enhanced by the small mass of the leptons. Our findings demonstrate the accessibility of these subleading resummation effects through the analysis of angular correlations in lepton pairs produced in UPCs at the Relativistic Heavy Ion Collider and the Large Hadron Collider.

DOI: 10.1103/PhysRevD.108.116015

I. INTRODUCTION

The study of pure electromagnetic dilepton production in ultraperipheral heavy ion collisions (UPCs) has been and continues to be an active area of research since the physics operation began at the Relativistic Heavy Ion Collider (RHIC) [1–11]. One of the key features of dilepton production in UPCs is the enhancement of the cross section by a factor of Z^4 at low transverse momentum, where Z is the nuclear charge number. This enhancement makes dilepton production in UPCs an attractive channel for searching for physics beyond the Standard Model [12–17], as well as for studying the properties of QED under extreme conditions [18–23].

Dilepton back-to-back production in the transverse plane in UPCs recently gained renewed interest from both experimental and theoretical sides. This is partially triggered by the observation of the lepton pair transverse momentum $q_\perp$ broadening at the Large Hadron Collider (LHC) [5,6,8] and RHIC [3,4]. The mean value of lepton pair transverse momentum was found to increase with decreasing impact parameter $b_\perp$ which is the transverse distance between two colliding nuclei. To account for this phenomenon, it is crucial to employ a formalism [10,24–31] that allows us to derive the joint $\boldsymbol{b}_\perp$ and $\boldsymbol{q}_\perp$ dependent cross section. As a result, the coherent photon distribution entering the cross section formula is the Wigner distribution rather than the transverse momentum dependent distribution.

In this paper, we focus on a relatively high pair transverse momentum region where the $q_\perp$ (>30 MeV) spectrum is no longer controlled by the primordial coherent photon distribution. The $q_\perp$ spectrum instead is dominantly generated via the recoiled effect due to the final state soft photon radiations when $q_\perp$ is much larger than the reverse of the nuclear radius. Despite the smallness of the QED fine-structure coupling constant α_e, the fixed order contribution is greatly enhanced by the large logarithm term of the type $\frac{\alpha_e}{\pi}\ln\frac{M^2}{m^2}\ln\frac{P_\perp^2}{q_\perp^2}$ and thus calls for a resummation, where M and m are the invariant mass of the lepton pair and lepton mass, respectively, and $P_\perp$ is approximately the individual lepton transverse momentum. Such a resummation formalism was first developed in the context of heavy quark pair production [32–35]. It later has been extended to include azimuthal dependent contributions [36,37] and applied to study azimuthal asymmetries in dilepton production in UPCs [37,38] in the leading double logarithm approximation. The first attempt to take into account the subleading logarithm contribution relevant in the kinematic region where m is of the same order as M to the azimuthal asymmetries in dimuon production has been presented in

Ref. [38]. The next to leading logarithm contribution to azimuthal asymmetries turns out to be sizable for muon production. The purpose of this work is to resum the subleading logarithm contribution in dielectron production, which is important in the kinematic limit $m \ll M$. Note that at low $q_\perp$ (~30 MeV), the azimuthal angular correlation in dilepton pair production mainly arises from the linear polarization of coherent photons [39–44] rather than the soft photon radiation effect.

In addition to directly measuring the $q_\perp$ distribution, the azimuthal angular decorrelation of the lepton pair is often studied experimentally. When the lepton pair acquires finite transverse momentum, either from the incoming coherent photons or from the recoiled effect due to soft photon radiation, the electron and positron are no longer produced in the exact back-to-back configuration in the transverse momentum phase space. The degree of the deviation from the back-to-back configuration is measured by the so-called acoplanarity, whose definition will be specified later. Acoplanarity as a way of exploring nucleon structure and quark gluon plasma (QGP) properties was extensively discussed in the context of dijet production and gauge boson-jet production [45–61]. The acoplanarity in dilepton production in UPCs was first studied in Refs. [27,62]. The leading double logarithm involved in the calculation of this observable is the type of $\frac{\alpha_e}{2\pi}\ln^2\frac{M^2}{q_x^2}$, where q_x is one of the transverse components of $\boldsymbol{q}_\perp$ perpendicular to $\boldsymbol{P}_\perp$. In this work, we extend the resummation formalism to the next to leading logarithm accuracy and investigate its phenomenological consequences as well.

The paper is structured as follows. We first briefly review the previous calculations for the observables under consideration in the next section. The resummation formalism formulated in the effective theory is discussed in Secs. II and III for two different kinds of angular correlations. The approach based on effective theory allows us to resum the subleading logarithm contribution to all orders in a systematic manner. We also present the heuristic derivations of the two Sudakov factors up to the next to leading logarithm accuracy following a more conventional perturbative QCD method in the Appendixes. The numerical results are presented in Sec. IV. We summarize the paper in Sec. V.

II. ANGULAR CORRELATIONS IN THE LEADING DOUBLE LOGARITHM APPROXIMATION

At low total transverse momentum of the dilepton pair, the electron and positron pair is dominantly produced via two coherent photon fusion processes. The corresponding kinematics are specified as follows:

$$\gamma_1(x_1 P + \tilde{k}_{1\perp}) + \gamma_2(x_2\bar{P} + \tilde{k}_{2\perp}) \to l^+(p_1) + l^-(p_2), \quad (1)$$

where P, $\bar{P}$, p_1, and p_2 are the four momenta of the two nucleons and final state leptons, respectively, $\tilde{k}_{1\perp} = (0,0,\boldsymbol{k}_{1\perp})$ and $\tilde{k}_{2\perp} = (0,0,\boldsymbol{k}_{2\perp})$ with $\boldsymbol{k}_{1\perp}$ and $\boldsymbol{k}_{2\perp}$ being the transverse momenta of the photons. The leptons are produced nearly back to back in azimuth with $q_\perp = |\boldsymbol{q}_\perp| \ll P_\perp = |\boldsymbol{P}_\perp|$, where the total transverse momentum $\boldsymbol{q}_\perp \equiv \boldsymbol{p}_{1\perp} + \boldsymbol{p}_{2\perp} = \boldsymbol{k}_{1\perp} + \boldsymbol{k}_{2\perp}$ and $\boldsymbol{P}_\perp = (\boldsymbol{p}_{1\perp} - \boldsymbol{p}_{2\perp})/2$. To sort out the UPC events, one has to first compute the impact parameter dependent cross section [24,63] and then integrate $b_\perp$ $(= |\boldsymbol{b}_\perp|)$ over the range $[2R_{\rm WS}, \infty)$, where $\boldsymbol{b}_\perp$ is the impact parameter between two colliding nuclei and $R_{\rm WS}$ is the nuclear radius. Once $\boldsymbol{b}_\perp$ dependence is introduced, the transverse momentum carried by the incoming photon in the amplitude is no longer identical to that in the conjugate amplitude. Below, we use $\boldsymbol{k}_{1\perp}, \boldsymbol{k}_{2\perp}$ and $\boldsymbol{k}'_{1\perp}, \boldsymbol{k}'_{2\perp}$ to denote transverse momenta in the amplitude and in the conjugate amplitude with the constraint $\boldsymbol{k}'_{1\perp} + \boldsymbol{k}'_{2\perp} \equiv \boldsymbol{q}_\perp$. The Born cross section of the dielectron production takes the form [39,40,64]

$$\frac{d\sigma_0}{d^2\boldsymbol{p}_{1\perp} d^2\boldsymbol{p}_{2\perp} dy_1 dy_2 d^2\boldsymbol{b}_\perp} = \frac{2\alpha_e^2}{M^4}\frac{1}{(2\pi)^2}[\mathcal{A} + \mathcal{B}\cos 2\phi + \mathcal{C}\cos 4\phi], \quad (2)$$

where ϕ is the angle between transverse momenta $\boldsymbol{q}_\perp$ and $\boldsymbol{P}_\perp$. y_1 and y_2 are lepton rapidities, respectively. M is the invariant mass of the lepton pair. At low $q_\perp$, the $\cos 4\phi$ azimuthal modulation is mainly induced by the linear polarization of coherent photons [39–44]. The computed $\cos 4\phi$ asymmetry [39,40] is in excellent agreement with the measured asymmetries by the STAR collaboration [41]. It is worth mentioning that the polarization dependent reactions in UPCs open a new avenue to explore the novel QCD phenomenology [65–72]. The hard coefficient $\mathcal{B}$ is suppressed by the power of $\frac{m^2}{M^2}$ at the tree level and is neglected. The coefficients $\mathcal{A}$ and $\mathcal{C}$ have been computed at the leading order in Ref. [40],

$$\mathcal{A} = \frac{M^2 - 2P_\perp^2}{P_\perp^2}\frac{Z^4\alpha_e^2}{\pi^4}\int d^2\boldsymbol{k}_{1\perp} d^2\boldsymbol{k}_{2\perp} d^2\boldsymbol{\Delta}_\perp \delta^2(\boldsymbol{q}_\perp - \boldsymbol{k}_{1\perp} - \boldsymbol{k}_{2\perp}) e^{i\boldsymbol{\Delta}_\perp\cdot\boldsymbol{b}_\perp}$$
$$\times [(\boldsymbol{k}_{1\perp}\cdot\boldsymbol{k}'_{1\perp})(\boldsymbol{k}_{2\perp}\cdot\boldsymbol{k}'_{2\perp}) + (\boldsymbol{k}_{1\perp}\cdot\boldsymbol{k}_{2\perp})\boldsymbol{\Delta}_\perp^2 - (\boldsymbol{k}_{1\perp}\cdot\boldsymbol{\Delta}_\perp)(\boldsymbol{k}_{2\perp}\cdot\boldsymbol{\Delta}_\perp)]$$
$$\times \mathcal{F}(x_1, \boldsymbol{k}_{1\perp}^2)\mathcal{F}^*(x_1, \boldsymbol{k}'^2_{1\perp})\mathcal{F}(x_2, \boldsymbol{k}_{2\perp}^2)\mathcal{F}^*(x_2, \boldsymbol{k}'^2_{2\perp}), \quad (3)$$

and

$$\mathcal{C} = -2\frac{Z^4\alpha_e^2}{\pi^4}\int d^2\boldsymbol{k}_{1\perp}d^2\boldsymbol{k}_{2\perp}d^2\boldsymbol{\Delta}_\perp\delta^2(\boldsymbol{q}_\perp-\boldsymbol{k}_{1\perp}-\boldsymbol{k}_{2\perp})e^{i\boldsymbol{\Delta}_\perp\cdot\boldsymbol{b}_\perp}$$
$$\times\{2[2(\boldsymbol{k}_{2\perp}\cdot\hat{\boldsymbol{q}}_\perp)(\boldsymbol{k}_{1\perp}\cdot\hat{\boldsymbol{q}}_\perp)-\boldsymbol{k}_{1\perp}\cdot\boldsymbol{k}_{2\perp}][2(\boldsymbol{k}'_{2\perp}\cdot\hat{\boldsymbol{q}}_\perp)(\boldsymbol{k}'_{1\perp}\cdot\hat{\boldsymbol{q}}_\perp)-\boldsymbol{k}'_{1\perp}\cdot\boldsymbol{k}'_{2\perp}]$$
$$-[(\boldsymbol{k}_{1\perp}\cdot\boldsymbol{k}'_{1\perp})(\boldsymbol{k}_{2\perp}\cdot\boldsymbol{k}'_{2\perp})+(\boldsymbol{k}_{1\perp}\cdot\boldsymbol{k}_{2\perp})\boldsymbol{\Delta}_\perp^2-(\boldsymbol{k}_{1\perp}\cdot\boldsymbol{\Delta}_\perp)(\boldsymbol{k}_{2\perp}\cdot\boldsymbol{\Delta}_\perp)]\}$$
$$\times\mathcal{F}(x_1,\boldsymbol{k}_{1\perp}^2)\mathcal{F}^*(x_1,\boldsymbol{k}'^2_{1\perp})\mathcal{F}(x_2,\boldsymbol{k}_{2\perp}^2)\mathcal{F}^*(x_2,\boldsymbol{k}'^2_{2\perp}), \tag{4}$$

where $\boldsymbol{\Delta}_\perp=\boldsymbol{k}_{1\perp}-\boldsymbol{k}'_{1\perp}=\boldsymbol{k}'_{2\perp}-\boldsymbol{k}_{2\perp}$. $\hat{\boldsymbol{q}}_\perp$ is a unit vector defined as $\hat{\boldsymbol{q}}=\boldsymbol{q}_\perp/q_\perp$. The incoming photons' longitudinal momentum fractions are fixed by the external kinematics according to $x_1=\sqrt{\frac{P_\perp^2+m^2}{s}}(e^{y_1}+e^{y_2})$ and $x_2=\sqrt{\frac{P_\perp^2+m^2}{s}}(e^{-y_1}+e^{-y_2})$ with m being the lepton mass and s being the square of the center-of-mass beam energy. $\mathcal{F}(x,\boldsymbol{k}_\perp^2)$ describes the amplitude of finding a photon carrying a certain momentum. For a given nuclear charge form factor $F(k^2)$, it is computed as $\mathcal{F}(x,\boldsymbol{k}_\perp^2)=\frac{F(\boldsymbol{k}_\perp^2+x^2M_p^2)}{(\boldsymbol{k}_\perp^2+x^2M_p^2)}$, where M_p is the proton mass. Note that the lepton mass is ignored in the hard coefficients.

At low transverse momentum $q_\perp$, the spectrum is primarily influenced by coherent photon distributions inherent to the primordial state, while at high $q_\perp$, the dominant contribution to the transverse momentum spectrum arises perturbatively from soft photon radiation in the final state. This latter effect is exacerbated by large logarithmic terms, necessitating an all-order resummation for accurate description. Such resummation is most conveniently performed in the transverse position space, as illustrated by the following expression:

$$\frac{d\sigma}{d^2\boldsymbol{p}_{1\perp}d^2\boldsymbol{p}_{2\perp}dy_1dy_2d^2\boldsymbol{b}_\perp}=\int\frac{d^2\boldsymbol{r}_\perp}{(2\pi)^2}e^{i\boldsymbol{r}_\perp\cdot\boldsymbol{q}_\perp}e^{-\mathrm{Sud}(r_\perp)}\times\int d^2\boldsymbol{q}'_\perp e^{-i\boldsymbol{r}_\perp\cdot\boldsymbol{q}'_\perp}\frac{d\sigma_0(\boldsymbol{q}'_\perp)}{d\mathcal{P}.\mathcal{S}.}, \tag{5}$$

where $r_\perp=|\boldsymbol{r}_\perp|$, $\mathrm{Sud}(r_\perp)$ represents the Sudakov factor, the phase space $d\mathcal{P}.\mathcal{S}.=d^2\boldsymbol{p}_{1\perp}d^2\boldsymbol{p}_{2\perp}dy_1dy_2d^2\boldsymbol{b}_\perp$, and $d\sigma_0(\boldsymbol{q}_\perp)\equiv d\sigma_0/d\boldsymbol{q}_\perp$. The leading logarithm contribution of the Sudakov factor has been derived in Refs. [32–34,36,37],

$$\mathrm{Sud}(r_\perp)=\frac{\alpha_e}{\pi}\ln\frac{M^2}{m^2}\ln\frac{P_\perp^2}{\mu_r^2}, \tag{6}$$

with $\mu_r=2e^{-\gamma_E}/r_\perp$. In this work, we extended the all-order Sudakov resummation to include the subleading logarithm contributions. The detailed derivations are presented in the next section (for a heuristic derivation, see Appendix A).

We now turn to discussing how to formulate the calculation of the acoplanarity. One can define an azimuthal angle $\phi_\perp=\pi-(\phi_1-\phi_2)$, where ϕ_1 and ϕ_2 represent the azimuthal angles for the lepton and the antilepton, respectively. The acoplanarity observed in experiments is defined as $\alpha=|\phi_\perp|/\pi$. We fix the direction of electron transverse momentum $\boldsymbol{p}_{1\perp}$ to be the Y axis. The acoplanarity can then be easily reconstructed by the ratio of q_x (the component of $\boldsymbol{q}_\perp$ aligned with the X axis) and $P_\perp$. The q_x dependent cross section takes the form

$$\begin{aligned}\frac{d\sigma}{dq_xd^2\boldsymbol{P}_\perp dy_1dy_2d^2\boldsymbol{b}_\perp}&=\int dq_y\frac{dr_ydr_x}{(2\pi)^2}e^{i(r_xq_x+r_yq_y)}e^{-\mathrm{Sud_a}(r_x,r_y)}\\&\quad\times\int dq'_xdq'_ye^{-i(r_xq'_x+r_yq'_y)}\frac{d\sigma_0(q'_\perp)}{d\mathcal{P}.\mathcal{S}.}\\&=\int\frac{dr_x}{2\pi}e^{ir_xq_x}e^{-\mathrm{Sud_a}(r_x,r_y=0)}\\&\quad\times\int dq'_xdq'_ye^{-ir_xq'_x}\frac{d\sigma_0(q'_\perp)}{d\mathcal{P}.\mathcal{S}.},\end{aligned} \tag{7}$$

where the leading logarithm contribution to the Sudakov factor $\mathrm{Sud_a}(r_x)$ is given by

$$\mathrm{Sud_a}(r_x)=\frac{\alpha_e}{2\pi}\left[\ln^2\frac{M^2}{\mu_{rx}^2}-\ln^2\frac{m^2}{\mu_{rx}^2}\theta(m-\mu_{rx})\right], \tag{8}$$

with $\mu_{rx}=2e^{-\gamma_E}/r_x$. This expression is identical to what is obtained in Ref. [62] if μ_{rx} is replaced with μ_r. One notices that we make a one-dimensional Fourier transform in the above-resummed formula rather than a two-dimensional Fourier transform as has been done in Eq. (5). This is because the acoplanarity is essentially a one-dimensional observable, whereas the $\boldsymbol{q}_\perp$ spectrum is a two-dimensional distribution. Naturally, the associated Sudakov factors in the two resummed cross sections differ from each other. When deriving the momentum space expression of the Sudakov factor $\mathrm{Sud_a}(l_x)$, the Y component of soft photon transverse momentum has to be integrated over the whole available phase-space region. It is thus not appropriate to reconstruct the q_x distribution from the resummed $\boldsymbol{q}_\perp$ distribution by integrating out q_y. We will present the detailed derivation of the Sudakov factor $\mathrm{Sud_a}(r_x)$ in Sec. IV (for a heuristic derivation, see Appendix B).

III. MASS FACTORIZATION AND RESUMMATION IN SCET

In the previous section, we presented the double logarithmic resummation formula for low transverse momentum $q_\perp$ and acoplanarity α. In this section, we will utilize the soft colliner effective theory (SCET) [73–77] and standard Renormalization Group (RG) methods to derive a resummation formula that includes the effects of lepton mass resummation to all orders. We adopt dimensional regularization in $d = 4 - 2\epsilon$ dimensions, following the $\overline{\mathrm{MS}}$ prescription. The dimensional regularization scale μ^2 is replaced by $\mu^2 e^{\gamma_E}/(4\pi)$, and we subtract ϵ poles to obtain the renormalized results in the $\overline{\mathrm{MS}}$ scheme. All renormalized results are presented in the $\overline{\mathrm{MS}}$ scheme.

A. Factorization formula at low $q_\perp$

In Ref. [38], we derived a resummation formula at low transverse momentum $q_\perp$ for muon pair production at the RHIC energy by assuming $M \sim m \gg q_\perp$. The differential cross section is factorized into the product of hard and soft factors, with the lepton mass m retained in both factors.

To obtain a resummation formula that includes lepton mass resummation, we need to refactorize the massive hard and soft functions in the small mass limit ($M \gg q_\perp \gtrsim m$). Explicitly, the massive hard function $H(M, m, \mu)$ is factorized as the product of the massless hard function $H(M, \mu)$ and collinear jet functions $J(m, \mu)$. Similarly, the massive soft function $S(l_\perp, \Delta y, m, \mu)$ is factorized as the product of the massless soft function $S(l_\perp, \Delta y, \mu)$ and collinear-soft functions $C_i(k_{i,\perp}, p_T, m, \mu)$. The resulting differential cross section is given by

$$\begin{aligned}\frac{d\sigma(q_\perp)}{d\mathcal{P.S.}} = {}& H(M,\mu) J^2(m,\mu) \int d^2\boldsymbol{l}_\perp d^2\boldsymbol{k}_{1\perp} d^2\boldsymbol{k}_{2\perp} \\ & \times \frac{d\sigma_0(|\boldsymbol{q}_\perp - \boldsymbol{l}_\perp - \boldsymbol{k}_{1\perp} - \boldsymbol{k}_{2\perp}|)}{d\mathcal{P.S.}} \\ & \times S(l_\perp, \Delta y, \mu) C_1(k_{1\perp}, P_\perp, y_1, m, \mu) \\ & \times C_2(k_{2\perp}, P_\perp, y_2, m, \mu), \end{aligned} \tag{9}$$

where the hard function $H(M, \mu)$ comes from the matching from QED to the low energy effective theory, and it can be obtained from the virtual corrections for massless amplitudes of $\gamma\gamma \to l^+ l^-$. The corresponding anomalous dimension is written as

$$\Gamma_H = \frac{\alpha_e}{4\pi}\left(8 \ln\frac{M^2}{\mu^2} - 12\right), \tag{10}$$

where the scale-dependent term gives double logarithmic resummation results, while the scale-independent term controls single logarithmic resummation. The physical scale in the hard function is $\mu_h = M$.

The collinear jet functions $J(m, \mu)$, which depend on the lepton mass, have been extensively studied in the literature [78–84]. In particular, the two-loop expression for these functions was derived in [85–87]. At the one-loop level, the jet function takes the form

$$\begin{aligned} J^{\mathrm{NLO}}(m,\mu) = 1 + \frac{\alpha_e}{4\pi}\Bigg[& \frac{2}{\epsilon^2} + \frac{1}{\epsilon}\left(1 + 2\ln\frac{\mu^2}{m^2}\right) \\ & + \left(1 + \ln\frac{\mu^2}{m^2}\right)\ln\frac{\mu^2}{m^2} + 4 + \frac{\pi^2}{6}\Bigg]. \end{aligned} \tag{11}$$

Then the one-loop anomalous dimension associated with this jet function is given by

$$\Gamma_J = \frac{\alpha_e}{4\pi}\left(4\ln\frac{\mu^2}{m^2} + 2\right). \tag{12}$$

It should be noted that the typical scale of the jet function is $\mu_j = m$, and that as matching coefficients of low energy effective theory, both hard and jet functions do not depend on the small transverse momentum.

The second line of Eq. (9) represents the factorization of the massive soft function in Ref. [38], which accounts for the contribution of real photon emissions. In the small m limit, the massless soft function S is defined in terms of soft Wilson lines,

$$S_{n_i}(x) = \exp\left[-ie\int_{-\infty}^{0} ds n_i\cdot A(x + s n_i)\right], \tag{13}$$

which describe a pointlike source traveling along the path $x^\mu + s n_i^\mu$ with the lightlike vector $n_i^2 = 0$. In the $r_\perp$ space we have the soft function

$$\tilde{S}(r_\perp, \Delta y) = \langle 0|\bar{\mathrm{T}}[S^\dagger_{n_1}(r_\perp) S_{n_2}(r_\perp)]\ \mathrm{T}[S^\dagger_{n_2}(0) S_{n_1}(0)]|0\rangle, \tag{14}$$

where $n_{1,2}$ denote the directions of final-state leptons. Expanding the Wilson line in the coupling perturbatively, the one-loop soft function is obtained as

$$\begin{aligned}\tilde{S}^{\mathrm{NLO}}(r_\perp, \Delta y) = 1 + e_0^2 \int & \frac{d^d k}{(2\pi)^{d-1}} \delta(k^2)\theta(k^0) \\ & \times \frac{2 n_1\cdot n_2}{n_1\cdot k k\cdot n_2} e^{i\boldsymbol{k}_\perp\cdot \boldsymbol{r}_\perp}, \end{aligned} \tag{15}$$

where e_0 is the bare electric charge, and k is the momentum of the final-state photon. Note that $\boldsymbol{k}_\perp$ is the photon transverse momentum with the beam directions which is different from the direction of n_i. After performing the momentum integral, we obtain

$$\tilde{S}^{\rm NLO}(r_\perp,\Delta y) = 1+\frac{\alpha_e}{4\pi}\left[\frac{4}{\epsilon^2}+\frac{4}{\epsilon}\ln\frac{\mu^2 r_\perp^2}{b_0^2 A_r}+2\ln^2\frac{\mu^2 r_\perp^2}{b_0^2 A_r}\right.$$
$$\left.+\pi^2-4\ln A_r\ln(1-A_r)-4{\rm Li}_2(A_r)\right], \tag{16}$$

where $b_0 = 2e^{-\gamma_E}$, $A_r = M^2/(4P_\perp^2\cos^2\phi_r)$ and ϕ_r represents the azimuthal angle of $\boldsymbol{r}_\perp$. In the $\boldsymbol{r}_\perp$ space μ_r is chosen as the soft scale, and the anomalous dimension is

$$\Gamma_S = \frac{\alpha_e}{4\pi}\left(8\ln\frac{\mu^2 r_\perp^2}{b_0^2}+8\ln\,\cos^2\phi_r-8\ln\frac{1+\cosh\Delta y}{2}\right). \tag{17}$$

It is apparent that as ϕ_r approaches $\pi/2$ or $3\pi/2$, i.e., when the direction of $r_\perp$ becomes perpendicular to the lepton direction, the expression becomes divergent due to the presence of ln $\cos^2\phi_r$. This divergence is connected to the rapidity divergence that dimensional regulators cannot regulate. We will elaborate on this further in the next subsection when we introduce the factorization formula for the acoplanarity distribution.

The soft function describes the large-angle long-wave photons contribution, while the collinear-soft function C_i captures the contribution from the soft photon radiating close to the lepton direction, which is defined as

$$\tilde{C}_i(r_\perp,P_\perp,y_i,m) = \langle 0|\bar{\rm T}[S^\dagger_{v_i}(r_\perp)S_{\bar{n}_i}(r_\perp)]\,{\rm T}[S^\dagger_{\bar{n}_i}(0)S_{v_i}(0)]|0\rangle, \tag{18}$$

where the soft Wilson line S_{v_i} is defined in analogy with S_{n_i} in Eq. (13), but with the lightlike vector n_i replaced with the timelike vector v_i, which is

$$v_i^\mu = \frac{\omega_i}{m}\frac{n_i^\mu}{2}+\frac{m}{\omega_i}\frac{\bar{n}_i^\mu}{2}, \quad \text{with} \quad \omega_i = 2P_\perp\cosh y_i. \tag{19}$$

At one loop, the perturbative expansion of the collinear-soft function gives us

$$\tilde{C}_i^{\rm NLO}(r_\perp,P_\perp,y_i,m) = 1+e_0^2\int\frac{d^dk}{(2\pi)^{d-1}}\delta(k^2)\theta(k^0)$$
$$\times\left(\frac{2v_i\cdot\bar{n}_i}{v_i\cdot k k\cdot\bar{n}_i}-\frac{v_i\cdot v_i}{v_i\cdot k k\cdot v_i}\right)$$
$$\times e^{i\bar{n}_i\cdot k n_i\cdot r_\perp/2}, \tag{20}$$

then we obtain

$$\tilde{C}_i^{\rm NLO}(r_\perp,P_\perp,y_i,m) = 1+\frac{\alpha_e}{4\pi}\left[-\frac{2}{\epsilon^2}+\frac{2}{\epsilon}(1-2\ln\mu R)\right.$$
$$\left.-4\ln^2\mu R+4\ln\mu R-\frac{5\pi^2}{6}\right], \tag{21}$$

where $R = -iP_\perp e^{\gamma_E}n_i\cdot r_\perp/(mr_\perp)$, and the anomalous dimension is

$$\Gamma_{C_{1,2}} = \frac{\alpha_e}{4\pi}\left(-4\ln\frac{4P_\perp^2\mu^2 r_\perp^2}{b_0^2 m^2}+4-4\ln\cos^2\phi_r\pm 4i\pi\right). \tag{22}$$

We set the collinear soft scale as $\mu_c = \mu_r m/(2P_\perp)$. With the anomalous dimensions presented for all the ingredients, we now show that our factorized formula satisfies the consistency relations for the RG evolutions. The consistency equation reads

$$\Gamma_H+\Gamma_S+2\Gamma_J+\Gamma_{C_1}+\Gamma_{C_2} = 0. \tag{23}$$

Based on the above discussions on the intrinsic scale and RG methods in SCET, we can obtain the expression for the all-order resummed cross section, and the Sudakov factor is given by

$${\rm Sud}(r_\perp) = \int_{\mu_r}^{M}\frac{d\mu}{\mu}\Gamma_H+2\int_{\mu_r}^{m}\frac{d\mu}{\mu}\Gamma_J+\int_{\mu_r}^{\mu_r m/(2P_\perp)}\frac{d\mu}{\mu}\Gamma_{C_1}$$
$$+\int_{\mu_r}^{\mu_r m/(2P_\perp)}\frac{d\mu}{\mu}\Gamma_{C_2}, \tag{24}$$

where we evolve hard, jet, and collinear-soft functions from their intrinsic scale to μ_r. After taking $\Delta y = 0$, and neglecting the contribution from single logarithmic terms, we find

$${\rm Sud}(r_\perp)|_{{\rm DL},\Delta y=0} = \frac{\alpha_e}{\pi}\ln\frac{M^2}{m^2}\ln\frac{P_\perp^2}{\mu_r^2}+\frac{\alpha_e}{\pi}\ln\frac{M^2}{m^2}\ln 4\cos^2\phi_r, \tag{25}$$

where the first term on the right is consistent with the Sudakov factor given in Eq. (6) [36–38]. In order to investigate the contributions from single logarithms, in the left panel of Fig. 1 we present the Sudakov factor for only double logarithmic terms and both double and single logarithmic terms. We find that the single logarithmic corrections reduce the Sudakov suppression.

Moreover, the azimuthal angle-dependent terms that are enhanced in the small mass limit are also resummed into an exponential form, and the azimuthal angle correlation coefficients are given by

$$A_2 \equiv \int_0^{2\pi}d\phi_r\frac{\cos 2\phi_r}{\pi}\exp\left(-\frac{\alpha_e}{\pi}\ln\frac{M^2}{m^2}\ln 4\cos^2\phi_r\right), \tag{26}$$

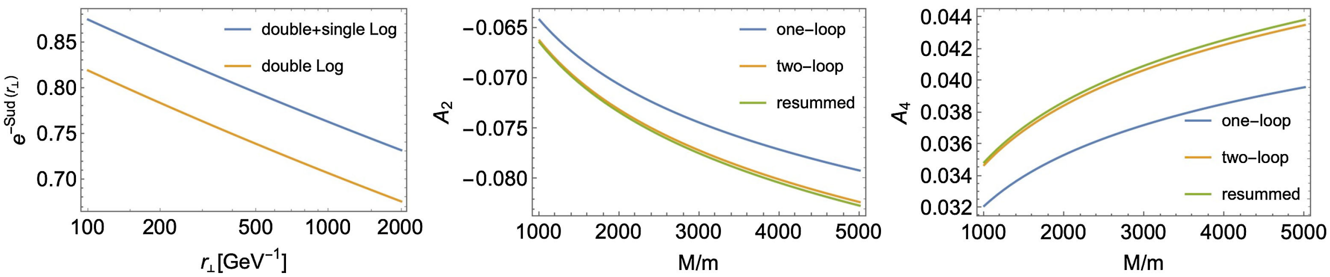

FIG. 1. Sudakov factor $\mathrm{Sud}(r_\perp)$ and azimuthal asymmetry $A_{2,4}$ in $q_\perp$ resummation formula. Left panel: Sudakov factor for double logarithmic (yellow line) and double + single logarithmic (blue line) contributions. The values of M, m, and Δy are chosen to be 500 MeV, 0.5 MeV, and 0, respectively. Middle panel: azimuthal asymmetry A_2 shown for leading order (blue), next-to-leading order (yellow), and all-order (green) results. Right panel: azimuthal asymmetry A_4 shown in the same colors as A_2.

$$A_4 \equiv \int_0^{2\pi} d\phi_r \frac{\cos 4\phi_r}{\pi} \exp\left(-\frac{\alpha_e}{\pi} \ln\frac{M^2}{m^2} \ln 4\cos^2\phi_r\right). \quad (27)$$

As a consistent check, we expand the above expression at one loop and find they reproduce the coefficients c_2 and c_4 in the limit $M \gg m$ [38] as follows:

$$A_2^{\mathrm{LO}} = -\frac{\alpha_e}{\pi} \ln\frac{M^2}{m^2} \int_0^{2\pi} d\phi_r \frac{\cos 2\phi_r}{\pi} \ln 4\cos^2\phi_r = -\frac{2\alpha_e c_2}{\pi}, \quad \text{with} \quad c_2 \approx \ln\frac{M^2}{m^2}, \quad (28)$$

$$A_4^{\mathrm{LO}} = -\frac{\alpha_e}{\pi} \ln\frac{M^2}{m^2} \int_0^{2\pi} d\phi_r \frac{\cos 4\phi_r}{\pi} \ln 4\cos^2\phi_r = \frac{\alpha_e c_4}{\pi}, \quad \text{with} \quad c_4 \approx \ln\frac{M^2}{m^2}, \quad (29)$$

where, as the azimuthal correlation first appears at one loop, we refer to the corresponding coefficients as the leading-order (LO) coefficients. Besides, we can use the all-order formula (25) to explore the azimuthal angular correlation coefficients at higher orders. The middle and right panels of Fig. 1 show $A_{2,4}$ at LO (one-loop), next to leading order (NLO) (two-loop), and all orders. It is evident that the high-order corrections enhance the azimuthal asymmetry, and the degree of enhancement depends on the scale hierarchy between M and m. In the typical RHIC kinematic regions, A_2 and A_4 increase by about 5% and 10%, respectively.

B. Factorization formula at low α

In the previous subsection, we derived a factorization formula for low values of $q_\perp$. Equations (17) and (22) show that the anomalous dimensions become divergent as the direction of $r_\perp$ becomes perpendicular to the lepton direction. If we choose that the direction of lepton transverse momentum is along the y axis and $r_\perp = r_x$, then the anomalous dimensions in Eqs. (17) and (22) diverge in dimensional regularization. As a result, we need to rederive a factorization formula in the small α limit since the acoplanarity α is reconstructed by q_x (or r_x in the conjugate Fourier space).

Since the hard and jet functions in Eq. (9) are matching coefficients that are independent of the specific observable, they should be the same in the factorization formula for the α distribution. In other words, only the soft and collinear-soft functions need to be modified in this case. As $\alpha \to 0$, the factorization formula should be expressed as

$$\frac{d\sigma(\alpha)}{d\mathcal{P.S.}} = 2P_\perp H(M,\mu) J^2(m,\mu) \int dl_x dk_{1,x} dk_{2,x} \times \frac{d\sigma_0(q_x - l_x - k_{1x} - k_{2x})}{d\mathcal{P.S.}} S(l_x, \Delta y, \mu, \nu) \times C_1(k_{1x}, P_\perp, y_1, m, \mu, \nu) \times C_2(k_{2x}, P_\perp, y_2, m, \mu, \nu), \quad (30)$$

where only a one-dimensional Fourier transformation is needed, as explained in Sec. II. The soft and collinear-soft functions exhibit different divergence structures from those in Eq. (9). Specifically, the naive separation of soft and collinear-soft momentum regions is not well defined without additional regulators. The modified factorization formula for the α distribution takes into account these extra divergences. The variable ν denotes the scale introduced by the dimensionless rapidity regulator. In this study, we will utilize the analytical regulator introduced in Refs. [88–90], and alternative regulators can be found in Refs. [91–97].

After performing the one-dimensional Fourier transformation, the operator definition of the soft function is given by

$$\tilde{S}(r_x, \Delta y) = \langle 0|\bar{\mathrm{T}}[S_{n_1}^\dagger(r_x) S_{n_2}(r_x)]\, \mathrm{T}[S_{n_2}^\dagger(0) S_{n_1}(0)]|0\rangle, \quad (31)$$

where r_x points along the x direction, which is perpendicular to the direction of the final state leptons in the y-z plane. The NLO soft function is therefore expressed as

$$\tilde{S}^{\mathrm{NLO}}(r_x, \Delta y) = 1 + e_0^2 \int \frac{d^d k}{(2\pi)^{d-1}} \delta(k^2)\theta(k^0) \left(\frac{\nu}{2k^0}\right)^\eta \times \frac{2n_1 \cdot n_2}{n_1 \cdot k k \cdot n_2} e^{ik_x r_x}, \quad (32)$$

where we introduce the rapidity regulator to regularize the rapidity divergence. In order to evaluate this integral, it is convenient to boost two lightlike vectors $n_{1,2}$ into their center-of-mass frame. Since such a boost operation can be performed in the y-z plane, the Fourier exponent function is not changed. As a result, only the rapidity regulator transforms as

$$\left(\frac{\nu}{2k^0}\right)^\eta \to \left(\frac{\nu}{2k^0}\sqrt{\frac{n_1\cdot n_2}{2}}\right)^\eta. \tag{33}$$

Therefore, we have the NLO soft function

$$\tilde{S}^{\rm NLO}(r_x,\Delta y) = 1+\frac{\alpha_e}{4\pi}\left[\frac{4}{\epsilon^2}-4\left(\ln\frac{\mu^2 r_x^2}{b_0^2}+\frac{1}{\epsilon}\right)\times\left(\frac{2}{\eta}+\ln\frac{n_1\cdot n_2\nu^2}{2\mu^2}\right)-2\ln^2\frac{\mu^2 r_x^2}{b_0^2}-\frac{\pi^2}{3}\right], \tag{34}$$

where the $1/\eta$ pole comes from rapidity divergences. In order to resum large logarithms associated with rapidity divergences, one can apply collinear anomaly [88,89] methods.

Similarly to the soft function, the operator definition of the collinear soft function takes the form

$$\tilde{C}_i(r_x,P_\perp,y_i,m) = \langle 0|\bar{\mathrm{T}}[S^\dagger_{v_i}(r_{\perp i})S_{\bar{n}_i}(r_{\perp i})]\ \mathrm{T}[S^\dagger_{\bar{n}_i}(0)S_{v_i}(0)]|0\rangle, \tag{35}$$

where $r_{\perp i}$ is perpendicular to the direction of the lepton. At one loop, we have

$$\tilde{C}_i^{\rm NLO}(r_{\perp i},P_\perp,y_i,m) = 1+e_0^2\int\frac{d^dk}{(2\pi)^{d-1}}\delta(k^2)\theta(k^0)\times\left(\frac{\nu}{\bar{n}_i\cdot k}\right)^\eta\left(\frac{2v_i\cdot\bar{n}_i}{v_i\cdot kk\cdot\bar{n}_i}-\frac{v_i\cdot v_i}{v_i\cdot kk\cdot v_i}\right)\times e^{ik_{\perp i}\cdot r_{\perp i}}, \tag{36}$$

where the small component of the momentum $n_i\cdot k$ in the rapidity regulator is expanded out and only the large component $\bar{n}_i\cdot k$ is retained since $2k^0 = n_i\cdot k+\bar{n}_i\cdot k$ in the light-cone coordinate. Therefore

$$\tilde{C}_i^{\rm NLO}(r_{\perp i},P_\perp,y_i,m) = 1+\frac{\alpha_e}{4\pi}\left[-\frac{2}{\epsilon^2}+\frac{2}{\epsilon}-2\left(\ln\frac{\mu^2 r_x^2}{b_0^2}+\frac{1}{\epsilon}\right)\times\left(\ln\frac{\omega_i^2\mu^2}{m^2\nu^2}-\frac{2}{\eta}\right)+\ln^2\frac{\mu^2 r_x^2}{b_0^2}+2\ln\frac{\mu^2 r_x^2}{b_0^2}+\frac{\pi^2}{6}\right]. \tag{37}$$

It is clear to see that the rapidity poles are canceled after combining soft and collinear-soft functions. Explicitly, we have

$$\tilde{S}\tilde{C}_1\tilde{C}_2 = 1+\frac{\alpha_e}{4\pi}\left(-4\ln\frac{\mu^2 r_x^2}{b_0^2}\ln\frac{M^2}{m^2}+4\ln\frac{\mu^2 r_x^2}{b_0^2}+8\pi^2\right)+\mathcal{O}(\alpha_e^2), \tag{38}$$

where the UV poles have been removed by the $\overline{\rm MS}$ subtraction scheme. Besides, the logarithm of the ratio between M and m cannot be resummed by standard RG equations, and this problem is referred to as the collinear anomaly, where the extra large logarithms are resummed by the collinear anomaly factor. Explicitly, we define

$$\tilde{S}\tilde{C}_1\tilde{C}_2 = \left(\frac{M^2}{m^2}\right)^{-F(r_x,\mu)}W(r_x,\mu), \tag{39}$$

where the anomaly exponent F depends only on r_x and the renormalization scale μ, and its one-loop expression is

$$F(r_x,\mu) = \frac{\alpha_e}{\pi}\ln\frac{\mu^2 r_x^2}{b_0^2}+\mathcal{O}(\alpha_e^2). \tag{40}$$

It satisfies the following RG equations:

$$\frac{d}{d\ln\mu}F(r_x,\mu) = \frac{2\alpha_e}{\pi}. \tag{41}$$

In Eq. (39) we have introduced the remainder function $W(r_x,\mu)$ which also depends only on r_x and μ,

$$W^{\rm NLO}(r_x,\mu) = 1+\frac{\alpha_e}{4\pi}\left(4\ln\frac{\mu^2 r_x^2}{b_0^2}+8\pi^2\right), \tag{42}$$

with the one-loop anomalous dimension as $\Gamma_W = 2\alpha_e/\pi$. The typical scale in F and W functions is μ_{rx}, and the RG consistency can be easily verified at one loop. After evolving the hard and jet functions to μ_{rx}, we obtain the all-order resummation formula for the α distribution, where the Sudakov factor is expressed as

$$\begin{aligned}\mathrm{Sud}_a(r_x) &= \int_{\mu_{rx}}^M\frac{d\mu}{\mu}\Gamma_H+2\int_{\mu_{rx}}^m\frac{d\mu}{\mu}\Gamma_J\theta(m-\mu_{rx}),\\ &= \frac{\alpha_e}{2\pi}\left[\left(\ln^2\frac{M^2}{\mu_{rx}^2}-3\ln\frac{M^2}{\mu_{rx}^2}\right)-\left(\ln^2\frac{m^2}{\mu_{rx}^2}-\ln\frac{m^2}{\mu_{rx}^2}\right)\theta(m-\mu_{rx})\right],\end{aligned} \tag{43}$$

where the double logarithmic terms are consistent with the expression in Eq. (8).

IV. NUMERICAL RESULTS

We now discuss the model input used in the numerical evaluations. It is convenient to perform the numerical calculation with the electromagnetic form factor taken from the STARlight MC generator [7],

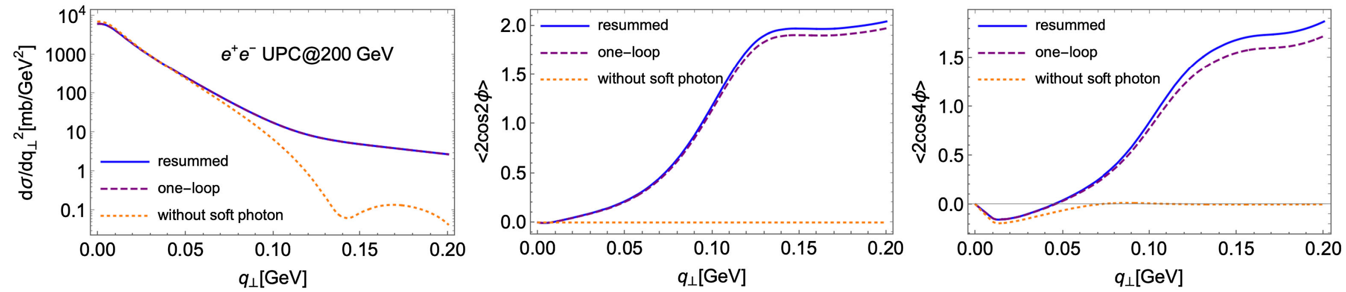

FIG. 2. Dielectron production in unrestricted UPCs in Au + Au collisions at the RHIC energy. The following kinematic cuts are imposed: the electrons' rapidities $|y_{1,2}| < 1$, transverse momentum $P_\perp > 200$ MeV, and the invariant mass of the electron pair 450 MeV $< M <$ 760 MeV. The blue solid lines stand for the fully resummed results from Eq. (24), and the purple dashed lines represent the results with the azimuthal dependent part being treated at the one-loop order. The results without soft photon radiation effect are shown with the dotted orange lines. Left panel: azimuthal averaged differential cross sections; middle panel: $\langle\cos(2\phi)\rangle$ azimuthal asymmetry; right panel: $\langle\cos(4\phi)\rangle$ azimuthal asymmetry.

$$F(|\boldsymbol{k}|) = \frac{4\pi\rho^0}{|\boldsymbol{k}|^3 A}[\sin(|\boldsymbol{k}|R_A) - |\boldsymbol{k}|R_A\cos(|\boldsymbol{k}|R_A)]\frac{1}{a^2|\boldsymbol{k}|^2+1}, \tag{44}$$

where $a = 0.7$ fm, and ρ^0 is a normalization factor. The nucleus radius is chosen to be $R_A = 1.1A^{1/3}$ fm for Au and Pb targets. This parametrization is numerically very close to the Woods-Saxon distribution.

The azimuthal asymmetries, i.e., the average value of $\cos 2n\phi$ are defined as

$$\langle\cos(2n\phi)\rangle = \frac{\int \frac{d\sigma}{d\mathcal{P}.\mathcal{S}.}\cos(2n\phi)d\mathcal{P}.\mathcal{S}.}{\int \frac{d\sigma}{d\mathcal{P}.\mathcal{S}.}d\mathcal{P}.\mathcal{S}.}. \tag{45}$$

We compute both the azimuthal independent cross sections and the asymmetries for the unrestricted UPC case, where we simply integrated the impact parameter over the range $[2R_{\rm WS}, \infty)$, with the nucleus radius $R_{\rm WS}$ being 6.4 fm for Au and 6.68 fm for Pb.

The azimuthal independent and dependent cross sections are plotted as a function of $q_\perp$ at RHIC energy in Fig. 2 and LHC energy in Fig. 3. It is clear to see that at relatively high $q_\perp$, the perturbative tail generated by soft photon radiation dominates over the lepton pair transverse momentum spectrum determined by the coherent photon primordial $k_\perp$ distribution. In this work, both the azimuthal independent and dependent leading logarithms are resummed into an exponential form, whereas in the previous work [36,37], we only resummed the azimuthal independent logarithm to all orders and treat the azimuthal dependent piece at the fixed order. We numerically compare the results computed from these two resummation schemes. The difference between these two methods becomes manifest when evaluating the azimuthal asymmetries in the large $q_\perp$ region, in particular for $\cos 4\phi$ azimuthal asymmetry. It would be interesting to test such a resummation effect in future experiments.

The acoplanarity distributions computed at LHC energy for both dielectron and dimuon production are displayed in Fig. 4. To avoid the possible contribution from incoherent photons, which could play a role in the large α region, we only make numerical estimations for the 0n0n events in which no neutron is emitted after the EM interaction

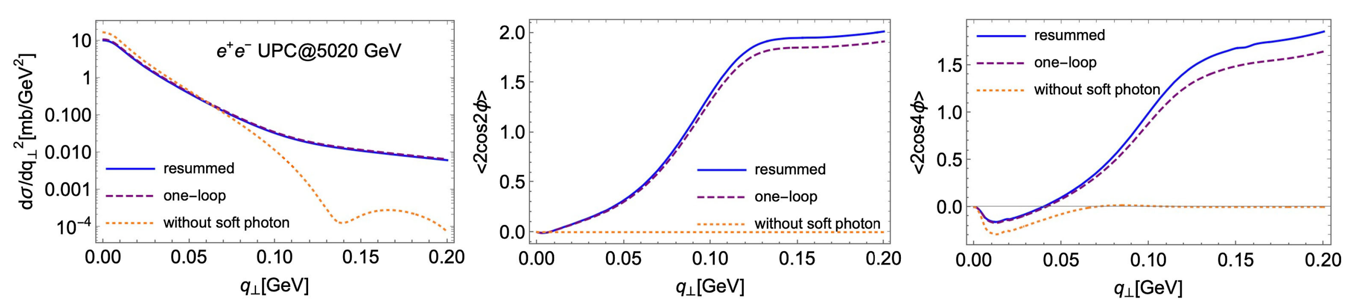

FIG. 3. Dielectron production in unrestricted UPCs in Pb + Pb collisions at the LHC energy. The following kinematic cuts are imposed: the electrons' rapidities $|y_{1,2}| < 0.8$ and the invariant mass of the dielectron 10 GeV $< M <$ 20 GeV. The blue solid lines stand for the fully resummed results from Eq. (24), and the purple dashed lines represent the results with the azimuthal dependent part being treated at the one-loop order. The results without soft photon radiation effect are shown with the dotted orange lines. Left panel: azimuthal averaged differential cross sections; middle panel: $\langle\cos(2\phi)\rangle$ azimuthal asymmetry; right panel: $\langle\cos(4\phi)\rangle$ azimuthal asymmetry.

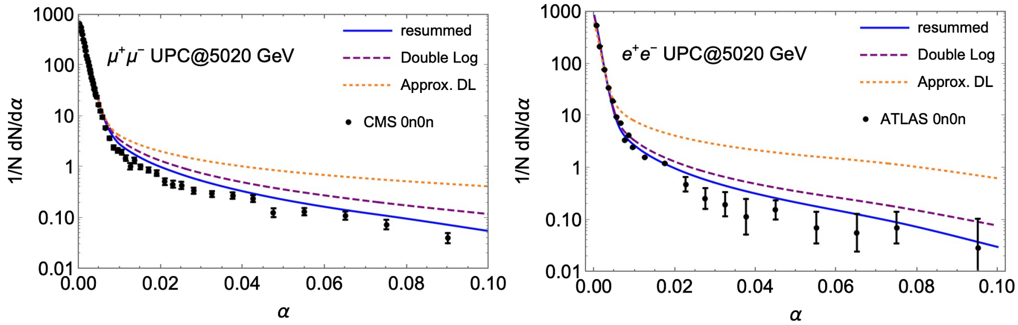

FIG. 4. The normalized cross sections of dilepton production are plotted as a function of α. Left panel: dimuon production in Pb + Pb collisions for the 0n0n case, with the kinematic cutoff: leptons' rapidities $|y_{1,2}| < 2.4$, transverse momentum $P_\perp > 3.5$ GeV, and the invariant mass of the dimuon 8 GeV $< M <$ 60 GeV. The CMS data displayed in the figure is taken from [99]. Right panel: dielectron production in Pb + Pb collisions for the 0n0n case, with the kinematic cutoff: leptons' rapidities $|y_{1,2}| < 0.8$ and the invariant mass of the dielectron 10 GeV $< M <$ 20 GeV. The ATLAS data shown in the figure is taken from [100]. The blue solid lines stand for the fully resummed results from Eq. (43), and the purple dashed lines represent the leading double logarithm resummed results obtained using Eq. (8). The acoplanarity distribution reconstructed from the resummed $q_\perp$ distribution given by Eqs. (5) and (6) is shown with the dotted orange lines.

occurs. For the 0n0n event, the impact parameter dependence of the cross section is weighted with an $b_\perp$ distribution (see the review article [98] and references therein),

$$2\pi \int_{2R_{\mathrm{WS}}}^{\infty} b_\perp db_\perp P^2(b_\perp) d\sigma(b_\perp, \ldots), \tag{46}$$

where the probability $P(b_\perp)$ for the 0n event is commonly parametrized as [18]

$$P(b_\perp) = \exp\left[-5.45 \times 10^{-5} \frac{Z^3(A-Z)}{A^{2/3} b_\perp^2}\right]. \tag{47}$$

The theoretical calculation is consistent with both ATLAS and CMS low α data. However, in the relatively large α region, our numerical results clearly overshoot the experimental data. The inclusion of the leading single logarithm contribution in the resummation formalism does relieve the tension between the experimental data and the theory calculation to some extent. The possible origin of this discrepancy is that collinear physics is not fully captured in our resummation formalism. The contribution from the phase-space region where the momentum of the emitted hard photon is almost aligned with that of the outgoing lepton is enhanced by a collinear logarithm. We can effectively resum such a large logarithm by introducing lepton fragmentation functions in our calculation, whose scale evolution is governed by the Dokshitzer-Gribov-Lipatov-Altarelli-Parisi (DGLAP) equation. We will address this point in future work. In the meantime, we also reconstruct the acoplanarity using the resummed $q_\perp$ distribution given in Eq. (5). The measured α distribution obviously does not favor this approach as shown in Fig. 4.

V. CONCLUSION

We study the azimuthal angular correlations of high-$q_\perp$ lepton pairs produced in UPCs, which are mainly generated by soft photon radiation in the final state. We show that the resummation of soft photon radiation has different formulations for the lepton pair $q_\perp$ distribution and the acoplanarity distribution, and that it is not valid to infer the acoplanarity distribution from the resummed $q_\perp$ distribution. Within the SCET framework, we perform the all-order resummation for both observables up to the single leading logarithm accuracy. Our results show that the $q_\perp$-dependent azimuthal asymmetries are not very sensitive to subleading resummation effects, but the leading single logarithm contribution is essential to describe the acoplanarity data from ATLAS and CMS. However, our calculations still exceed the data for large α. This discrepancy certainly warrants further investigation. Nevertheless, we conclude that the process of lepton pair production in UPCs provides a great opportunity to test the resummation formalism through angular correlations, thanks to the high coherent photon luminosity and the high angular resolution of modern detectors [101]. The resummation formalism presented here can be extended to study the angular correlations in the diffractive productions of dijet, jet-hadron, and hadron-hadron in UPCs. We leave these for future studies.

ACKNOWLEDGMENTS

We thank Chi Yang, Shuai Yang, Xiao-feng Wang and Tianbo Liu for their helpful discussions. D. Y. S. is supported by the National Science Foundations of China under Grants No. 12275052 and No. 12147101 and the Shanghai Natural Science Foundation under Grant No. 21ZR1406100. J. Zhou has been supported by the National Science Foundations of China under Grant

No. 12175118. Y. Zhou has been supported by the Natural Science Foundation of Shandong Province under Grant No. ZR2020MA098. C. Zhang has been supported by the National Science Foundations of China under Grant No. 12147125.

APPENDIX A: A HEURISTIC DERIVATION OF THE SUDAKOV FACTOR Sud$(r_\perp)$

The subleading logarithm contribution to the Sudakov factor Sud$(r_\perp)$ can be derived in an alternative way. We start by discussing the azimuthal angular dependent part. The soft factor in the leading logarithm approximation can be expanded as [37]

$$S(l_\perp) = \frac{\alpha_e}{\pi^2}\frac{1}{l_\perp^2}\ln\frac{M^2}{m^2}\{1 + 2\cos 2\phi + 2\cos 4\phi + 2\cos 6\phi + \cdots\}, \tag{A1}$$

where ϕ is the azimuthal angle between the soft photon transverse momentum $l_\perp$ and $P_\perp$. Our task is to Fourier transform the soft factor to $r_\perp$ space $S(r_\perp) = \int d^2 l_\perp e^{i r_\perp \cdot l_\perp} S(l_\perp)$. With the help of the Jacobi-Anger expansion,

$$e^{iz\cos(\phi)} = J_0(z) + 2\sum_{n=1}^{\infty} i^n J_n(z)\cos(n\phi), \tag{A2}$$

and the integration formula,

$$\int_0^\infty \frac{d|q'_\perp|}{|q'_\perp|} J_n(|q'_\perp||b_\perp|) = \frac{1}{n}, \tag{A3}$$

one arrives at

$$S(r_\perp) = \frac{\alpha_e}{\pi}\ln\frac{M^2}{m^2} 4\sum_{n=1}^{\infty}\frac{i^{2n}}{2n}\cos(2n\phi_r) = -\frac{\alpha_e}{\pi}\ln\frac{M^2}{m^2}\ln[2 + 2\cos(2\phi_r)], \tag{A4}$$

where ϕ_r is the azimuthal angle between $r_\perp$ and $P_\perp$. This result is consistent with the second term in Eq. (25).

Now we turn to discuss the derivation of the single logarithm terms. For simplicity, we consider the special case $\Delta y = 0$. The part of the single logarithm contribution purely comes from the virtual correction. The leading logarithm virtual correction can be expressed as (see, for example, [102,103])

$$\frac{\alpha_e}{2\pi^2}\int_0^M \frac{d^2 l_\perp}{l_\perp^2 + \frac{(1-z)^2}{z^2}m^2}\int dz \frac{1+z^2}{1-z}, \tag{A5}$$

in the frame where the electron momentum is chosen to be the light-cone direction. z stands for the longitudinal momentum fraction of the electron carried by the virtual photon. The UV cutoff is chosen to be the lepton pair invariant mass. The virtual contribution from the soft region has already been combined with the real correction to form the leading double logarithm contribution. Therefore, we have to subtract the soft region contribution,

$$\frac{\alpha_e}{2\pi^2}\int_0^M \frac{d^2 l_\perp}{l_\perp^2 + \frac{(1-z)^2}{z^2}m^2}\int dz\left[\frac{1+z^2}{1-z} - \frac{2}{1-z}\right] = \frac{3}{4}\frac{\alpha_e}{\pi}\ln\frac{M^2}{m^2} + \mathcal{O}\left(\frac{1}{\ln\frac{M^2}{m^2}}\right). \tag{A6}$$

Another contribution to the single logarithm term is from the diagram where a soft photon connects two electron lines or two positron lines. After applying the Eikonal approximation, one has

$$\int \frac{d^3 q}{2q^0}\frac{m^2}{(q\cdot P)^2} = \int \frac{dq_\perp^2}{4q_\perp^2 P_\perp^2}\int dy d\phi \times \frac{m^2}{\left[\sqrt{1+\frac{m^2}{P_\perp^2}}\cosh(y) - \cos\phi\right]^2} = \int \frac{dq_\perp^2}{4q_\perp^2 P_\perp^2}\int dy \frac{m^2 2\pi\sqrt{1+\frac{m^2}{P_\perp^2}}\cosh(y)}{\left[\left(1+\frac{m^2}{P_\perp^2}\right)\cosh^2(y) - 1\right]^{\frac{3}{2}}}. \tag{A7}$$

After changing the variable $e^y = z$, the above y integration can be readily carried out,

$$e^2\int \frac{d^3 q}{(2\pi)^3 2q^0}\frac{m^2}{(q\cdot P)^2} \approx \frac{\alpha_e}{2\pi^2}\int \frac{d^2 q_\perp}{q_\perp^2}, \tag{A8}$$

where the terms suppressed by the power of $m^2/P_\perp^2$ have been neglected. Now we combine the virtual and real corrections together,

$$\frac{\alpha_e}{2\pi^2}\int^M \frac{d^2 q_\perp}{q_\perp^2}(1 - e^{i q_\perp \cdot r_\perp}) \approx \frac{\alpha_e}{2\pi}\ln\frac{M^2}{\mu_r^2}. \tag{A9}$$

The sum of Eqs. (A6) and (A9) gives the full single logarithm contribution from each lepton line to the Sudakov factor Sud$(r_\perp)$.

APPENDIX B: A HEURISTIC DERIVATION OF THE SUDAKOV FACTOR Sud$_\mathrm{a}(r_x)$

The Sudakov factor Sud$_\mathrm{a}(r_x)$ can be reproduced by isolating the large logarithm contributions from the collinear splitting function for the electron. In the collinear limit, the electron fragmentation function at the leading order reads (see, for example, [102,103])

$$\frac{\alpha_e}{2\pi^2}\int_0^M \frac{d^2 l_\perp}{l_\perp^2+\frac{(1-z)^2}{z^2}m^2}\int dz\frac{1+z^2}{1-z} + \text{virtual correction}, \tag{B1}$$

where $l_\perp$ is perpendicular to the outgoing electron momentum p_1. The X component of $l_\perp$, i.e., l_x, is chosen such that it satisfies the following conditions:

$$p_2\cdot l_x = 0,\quad p_{2\perp}\cdot l_x = 0,\quad p\cdot l_x = 0,\quad n\cdot l_x = 0, \tag{B2}$$

where p^μ and n^μ are the commonly defined light-cone vectors along the beam direction in the lab frame. The acoplanarity is determined by the ratio of l_x and $p_{2\perp} = p_{2\perp,y}$ where p_2 is positron momentum. Since l_y goes unobserved, it needs to be integrated out at the end of the calculations. Note that l_y is generally not perpendicular to the light-cone momenta p^μ and n^μ.

The light-cone divergence $z\to 1$ in Eq. (B1) can be cured by taking into account the exact kinematics. According to the on-shell condition of a radiated photon, one has

$$\frac{l_\perp^2}{2\bar{P}^-} < l^+ < P^+, \tag{B3}$$

where P^+ and $\bar{P}^-$ stand for the light-cone vectors along the lepton momentum direction instead of these along the beam direction. We take the collinear photon emission along the P^+ direction as an example. To avoid double counting, we further require

$$l^- < l^+, \tag{B4}$$

which leads to the constraint

$$\frac{\sqrt{2}|l_\perp|}{2} < l^+ < P^+. \tag{B5}$$

This converts to the integration limits for z which are specified as

$$\begin{aligned}
&\frac{\alpha_e}{2\pi^2}\int_0^M \frac{d^2 l_\perp}{l_\perp^2+\frac{(1-z)^2}{z^2}m^2}\int_0^{1-\frac{\sqrt{2}}{2}\frac{l_\perp}{P^+}} dz\frac{1+z^2}{1-z}\\
&\approx \frac{\alpha_e}{2\pi^2}\int_0^M d^2 l_\perp\Bigg[\int_0^1 dz\frac{1}{l_\perp^2+\frac{(1-z)^2}{z^2}m^2}\frac{1+z^2}{(1-z)_+}\\
&\quad+\int_0^{1-\sqrt{\frac{l_\perp^2}{M^2}}} dz\frac{1}{l_\perp^2+\frac{(1-z)^2}{z^2}m^2}\frac{2}{1-z}\Bigg]\\
&\approx \frac{\alpha_e}{2\pi^2}\int_0^1 dz\int_0^M \frac{d^2 l_\perp}{l_\perp^2}\frac{1+z^2}{(1-z)_+}\\
&\quad+\frac{\alpha_e}{2\pi^2}\int_0^M \frac{d^2 l_\perp}{l_\perp^2}\ln\frac{m^2+M^2}{l_\perp^2+m^2}.
\end{aligned}\tag{B6}$$

The term in the fifth line gives rises to the leading double logarithm contribution. Combining with the virtual correction, one has

$$\begin{aligned}
&\int_0^M \frac{d^2 l_\perp}{l_\perp^2}\ln\frac{M^2}{l_\perp^2+m^2}[e^{il_\perp\cdot r_\perp}-1]\\
&=\int_0^M \frac{d^2 l_\perp}{l_\perp^2}\left\{\ln\frac{M^2}{l_\perp^2}+\ln\frac{l_\perp^2}{l_\perp^2+m^2}\right\}[e^{il_\perp\cdot r_\perp}-1].
\end{aligned}\tag{B7}$$

As explained earlier, we should only make the Fourier transform with respect to l_x, and integrated out l_y. The integration over l_y can be easily achieved by setting $r_y=0$ at the end of the calculations. It is straightforward to carry out $l_\perp$ integration,

$$\int_0^M \frac{d^2 l_\perp}{l_\perp^2}\ln\frac{M^2}{l_\perp^2}[e^{il_\perp\cdot r_\perp}-1]\approx -\frac{\pi}{2}\ln^2\frac{M^2}{\mu_r^2}, \tag{B8}$$

and

$$\int_0^M \frac{d^2 l_\perp}{l_\perp^2}\ln\frac{l_\perp^2}{l_\perp^2+m^2}[e^{il_\perp\cdot r_\perp}-1]\approx -\frac{\pi}{2}\ln^2\frac{m^2}{\mu_r^2}\theta(m-\mu_r), \tag{B9}$$

where we only keep the leading logarithm contributions. After carrying out l_y integration, r_y is fixed to be 0. Correspondingly, μ_r is converted into μ_x. These two double logarithm terms can be promoted to an exponential form after carrying out all-order resummation.

Now we consider the collinear part that is free of the light-cone divergence,

$$\begin{aligned}
&\frac{\alpha_e}{2\pi^2}\frac{1}{l_\perp^2}\frac{1+z^2}{(1-z)_+}-\frac{\alpha_e}{2\pi^2}\delta^2(l_\perp)\delta(1-z)\\
&\quad\times\int\frac{d^2 k_\perp}{k_\perp^2}\int_0^1 d\xi\frac{1+\xi^2}{(1-\xi)_+}\\
&=\frac{\alpha_e}{2\pi^2}\frac{1}{l_\perp^2}\left[\frac{1+z^2}{(1-z)_+}+\frac{3}{2}\delta(1-z)\right]\\
&\quad-\frac{\alpha_e}{2\pi^2}\frac{3}{2}\delta(1-z)\left[\frac{1}{l_\perp^2}-\delta^2(l_\perp)\int\frac{d^2 k_\perp}{k_\perp^2}\right],
\end{aligned}\tag{B10}$$

where it is safe to neglect $\frac{(1-z)^2}{z^2}m^2$ in the denominator as the integration is no longer dominated by the region $z\to 1$. The last two terms proportional to $\delta(1-z)$ can be resummed into an exponential form after making the Fourier transform. In $r_\perp$ space, it reads

$$-\delta(1-z)\frac{\alpha_e}{2\pi^2}\frac{3}{2}\int_0^M\frac{d^2 l_\perp}{l_\perp^2}(e^{ir_\perp\cdot l_\perp}-1)=\delta(1-z)\frac{\alpha_e}{2\pi}\frac{3}{2}\ln\frac{M^2}{\mu_r^2}, \tag{B11}$$

which contributes to the single leading logarithm term in the Sudakov factor $\mathrm{Sud_a}(r_x)$. The term involving the DGLAP splitting kernel in Eq. (B10) should be absorbed into the renormalized electron fragmentation function. Another single logarithm term $\frac{\alpha_e}{2\pi}\ln\frac{m^2}{\mu_r^2}\theta(m-\mu_r)$ receives the contribution from the diagrams with the soft photon connecting two electron lines or two positron lines in the cutting graphs. The derivation of this term is rather straightforward. We thus reproduce both the double and the single logarithm terms in the Sudakov factor $\mathrm{Sud_a}(r_x)$ given in Eq. (43).

---

[1] A. J. Baltz, Phys. Rep. **458**, 1 (2008).
[2] C. A. Bertulani, S. R. Klein, and J. Nystrand, Annu. Rev. Nucl. Part. Sci. **55**, 271 (2005).
[3] J. Adam *et al.* (STAR Collaboration), Phys. Rev. Lett. **121**, 132301 (2018).
[4] J. Adam *et al.* (STAR Collaboration), arXiv:1810.10159.
[5] M. Aaboud *et al.* (ATLAS Collaboration), Phys. Rev. Lett. **121**, 212301 (2018).
[6] S. Acharya *et al.* (ALICE Collaboration), Phys. Rev. C **99**, 024002 (2019).
[7] S. R. Klein, J. Nystrand, J. Seger, Y. Gorbunov, and J. Butterworth, Comput. Phys. Commun. **212**, 258 (2017).
[8] ALICE Collaboration, CERN Report No. ALICE-PUBLIC-2022-007, 2022.
[9] J. Zhou (STAR Collaboration), EPJ Web Conf. **259**, 13014 (2022).
[10] X. Wang, J. D. Brandenburg, L. Ruan, F. Shao, Z. Xu, C. Yang, and W. Zha, Phys. Rev. C **107**, 044906 (2023).
[11] P.-Y. Niu, E. Wang, Q. Wang, and S. Yang, arXiv:2209.01924.
[12] J. Abdallah *et al.* (DELPHI Collaboration), Eur. Phys. J. C **35**, 159 (2004).
[13] ATLAS Collaboration, Phys. Rev. Lett. **131**, 151802 (2023).
[14] S. Knapen, T. Lin, H. K. Lou, and T. Melia, Phys. Rev. Lett. **118**, 171801 (2017).
[15] A. M. Sirunyan *et al.* (CMS Collaboration), Phys. Lett. B **797**, 134826 (2019).
[16] J. Ellis, N. E. Mavromatos, and T. You, Phys. Rev. Lett. **118**, 261802 (2017).
[17] I. Xu, N. Lewis, X. Wang, J. D. Brandenburg, and L. Ruan, arXiv:2211.02132.
[18] G. Baur, K. Hencken, and D. Trautmann, J. Phys. G **24**, 1657 (1998).
[19] S. Klein and P. Steinberg, Annu. Rev. Nucl. Part. Sci. **70**, 323 (2020).
[20] P. A. Steinberg, Nucl. Phys. **A1005**, 122007 (2021).
[21] K. Hattori, H. Taya, and S. Yoshida, J. High Energy Phys. 01 (2021) 093.
[22] P. Copinger and S. Pu, Int. J. Mod. Phys. A **35**, 2030015 (2020).
[23] J. D. Brandenburg, W. Zha, and Z. Xu, Eur. Phys. J. A **57**, 299 (2021).
[24] M. Vidovic, M. Greiner, C. Best, and G. Soff, Phys. Rev. C **47**, 2308 (1993).
[25] K. Hencken, D. Trautmann, and G. Baur, Phys. Rev. A **51**, 1874 (1995).
[26] W. Zha, J. D. Brandenburg, Z. Tang, and Z. Xu, Phys. Lett. B **800**, 135089 (2020).
[27] S. Klein, A. H. Mueller, B.-W. Xiao, and F. Yuan, Phys. Rev. D **102**, 094013 (2020).
[28] R.-j. Wang, S. Pu, and Q. Wang, Phys. Rev. D **104**, 056011 (2021).
[29] R.-j. Wang, S. Lin, S. Pu, Y.-f. Zhang, and Q. Wang, Phys. Rev. D **106**, 034025 (2022).
[30] S. Lin, R.-J. Wang, J.-F. Wang, H.-J. Xu, S. Pu, and Q. Wang, Phys. Rev. D **107**, 054004 (2023).
[31] M. Klusek-Gawenda, W. Schäfer, and A. Szczurek, Phys. Lett. B **814**, 136114 (2021).
[32] H. X. Zhu, C. S. Li, H. T. Li, D. Y. Shao, and L. L. Yang, Phys. Rev. Lett. **110**, 082001 (2013).
[33] H. T. Li, C. S. Li, D. Y. Shao, L. L. Yang, and H. X. Zhu, Phys. Rev. D **88**, 074004 (2013).
[34] S. Catani, M. Grazzini, and A. Torre, Nucl. Phys. **B890**, 518 (2014).
[35] W.-L. Ju and M. Schönherr, J. High Energy Phys. 02 (2023) 075.
[36] Y. Hatta, B.-W. Xiao, F. Yuan, and J. Zhou, Phys. Rev. Lett. **126**, 142001 (2021).
[37] Y. Hatta, B.-W. Xiao, F. Yuan, and J. Zhou, Phys. Rev. D **104**, 054037 (2021).
[38] D. Y. Shao, C. Zhang, J. Zhou, and Y. Zhou, Phys. Rev. D **107**, 036020 (2023).
[39] C. Li, J. Zhou, and Y.-J. Zhou, Phys. Lett. B **795**, 576 (2019).
[40] C. Li, J. Zhou, and Y.-J. Zhou, Phys. Rev. D **101**, 034015 (2020).
[41] J. Adam *et al.* (STAR Collaboration), Phys. Rev. Lett. **127**, 052302 (2021).
[42] B.-W. Xiao, F. Yuan, and J. Zhou, Phys. Rev. Lett. **125**, 232301 (2020).
[43] J. Zhao, J. Chen, X.-G. Huang, and Y.-G. Ma, arXiv:2211.03968.
[44] J. D. Brandenburg, J. Seger, Z. Xu, and W. Zha, Rep. Prog. Phys. **86**, 083901 (2023).
[45] A. Banfi, M. Dasgupta, and Y. Delenda, Phys. Lett. B **665**, 86 (2008).
[46] F. Hautmann and H. Jung, J. High Energy Phys. 10 (2008) 113.
[47] L. Zheng, E. C. Aschenauer, J. H. Lee, and B.-W. Xiao, Phys. Rev. D **89**, 074037 (2014).
[48] P. Sun, C. P. Yuan, and F. Yuan, Phys. Rev. Lett. **113**, 232001 (2014).
[49] P. Sun, C. P. Yuan, and F. Yuan, Phys. Rev. D **92**, 094007 (2015).
[50] L. Chen, G.-Y. Qin, L. Wang, S.-Y. Wei, B.-W. Xiao, H.-Z. Zhang, and Y.-Q. Zhang, Nucl. Phys. **B933**, 306 (2018).

[51] P. Sun, B. Yan, C. P. Yuan, and F. Yuan, Phys. Rev. D **100**, 054032 (2019).
[52] X. Liu, F. Ringer, W. Vogelsang, and F. Yuan, Phys. Rev. Lett. **122**, 192003 (2019).
[53] Y.-T. Chien, D. Y. Shao, and B. Wu, J. High Energy Phys. 11 (2019) 025.
[54] X. Liu, F. Ringer, W. Vogelsang, and F. Yuan, Phys. Rev. D **102**, 094022 (2020).
[55] Y.-T. Chien, R. Rahn, S. Schrijnder van Velzen, D. Y. Shao, W. J. Waalewijn, and B. Wu, Phys. Lett. B **815**, 136124 (2021).
[56] M. I. Abdulhamid *et al.*, Eur. Phys. J. C **82**, 36 (2022).
[57] Y.-T. Chien, R. Rahn, D. Y. Shao, W. J. Waalewijn, and B. Wu, J. High Energy Phys. 02 (2023) 256.
[58] H. Bouaziz, Y. Delenda, and K. Khelifa-Kerfa, J. High Energy Phys. 10 (2022) 006.
[59] H. Yang *et al.*, Eur. Phys. J. C **82**, 755 (2022).
[60] A. B. Martinez and F. Hautmann, in *29th International Workshop on Deep-Inelastic Scattering and Related Subjects* (2022); arXiv:2208.08446.
[61] C. Zhang, Q.-S. Dai, and D. Y. Shao, J. High Energy Phys. 02 (2020) 002.
[62] S. Klein, A. Mueller, B.-W. Xiao, and F. Yuan, Phys. Rev. Lett. **122**, 132301 (2019).
[63] K. Hencken, D. Trautmann, and G. Baur, Phys. Rev. A **49**, 1584 (1994).
[64] C. Pisano, D. Boer, S. J. Brodsky, M. G. A. Buffing, and P. J. Mulders, J. High Energy Phys. 10 (2013) 024.
[65] Y. Hagiwara, C. Zhang, J. Zhou, and Y.-J. Zhou, Phys. Rev. D **103**, 074013 (2021).
[66] H. Xing, C. Zhang, J. Zhou, and Y.-J. Zhou, J. High Energy Phys. 10 (2020) 064.
[67] Y. Hagiwara, C. Zhang, J. Zhou, and Y.-j. Zhou, Phys. Rev. D **104**, 094021 (2021).
[68] J. D. Brandenburg, Z. Xu, W. Zha, C. Zhang, J. Zhou, and Y. Zhou, Phys. Rev. D **106**, 074008 (2022).
[69] H. Mäntysaari, F. Salazar, and B. Schenke, Phys. Rev. D **106**, 074019 (2022).
[70] X. Wu, X. Li, Z. Tang, P. Wang, and W. Zha, Phys. Rev. Res. **4**, L042048 (2022).
[71] M. Abdallah *et al.* (STAR Collaboration), Sci. Adv. **9**, eabq3903 (2023).
[72] W. Zha, J. D. Brandenburg, L. Ruan, Z. Tang, and Z. Xu, Phys. Rev. D **103**, 033007 (2021).
[73] C. W. Bauer, S. Fleming, D. Pirjol, and I. W. Stewart, Phys. Rev. D **63**, 114020 (2001).
[74] C. W. Bauer and I. W. Stewart, Phys. Lett. B **516**, 134 (2001).
[75] C. W. Bauer, D. Pirjol, and I. W. Stewart, Phys. Rev. D **65**, 054022 (2002).
[76] C. W. Bauer, S. Fleming, D. Pirjol, I. Z. Rothstein, and I. W. Stewart, Phys. Rev. D **66**, 014017 (2002).
[77] M. Beneke, A. P. Chapovsky, M. Diehl, and T. Feldmann, Nucl. Phys. **B643**, 431 (2002).
[78] M. Neubert, arXiv:0706.2136.
[79] A. Ferroglia, S. Marzani, B. D. Pecjak, and L. L. Yang, J. High Energy Phys. 01 (2014) 028.
[80] C. W. Bauer and E. Mereghetti, J. High Energy Phys. 04 (2014) 051.
[81] M. Fickinger, S. Fleming, C. Kim, and E. Mereghetti, J. High Energy Phys. 11 (2016) 095.
[82] Z.-B. Kang, J. Reiten, D. Y. Shao, and J. Terry, J. High Energy Phys. 05 (2021) 286.
[83] D. Gaggero, A. Ghira, S. Marzani, and G. Ridolfi, J. High Energy Phys. 09 (2022) 058.
[84] R. von Kuk, J. K. L. Michel, and Z. Sun, J. High Energy Phys. 09 (2023) 205.
[85] A. Mitov and S. Moch, J. High Energy Phys. 05 (2007) 001.
[86] T. Becher and K. Melnikov, J. High Energy Phys. 06 (2007) 084.
[87] A. Jain, I. Scimemi, and I. W. Stewart, Phys. Rev. D **77**, 094008 (2008).
[88] T. Becher and M. Neubert, Eur. Phys. J. C **71**, 1665 (2011).
[89] T. Becher and G. Bell, Phys. Lett. B **713**, 41 (2012).
[90] G. Bell, R. Rahn, and J. Talbert, J. High Energy Phys. 07 (2019) 101.
[91] J. Collins, *Foundations of Perturbative QCD* (Cambridge University Press, Cambridge, England, 2013), Vol. 32, ISBN 978-1-107-64525-7, 978-1-107-64525-7, 978-0-521-85533-4, 978-1-139-09782-6.
[92] M. G. Echevarria, A. Idilbi, and I. Scimemi, J. High Energy Phys. 07 (2012) 002.
[93] M. G. Echevarría, A. Idilbi, and I. Scimemi, Phys. Lett. B **726**, 795 (2013).
[94] J.-y. Chiu, A. Jain, D. Neill, and I. Z. Rothstein, Phys. Rev. Lett. **108**, 151601 (2012).
[95] J.-Y. Chiu, A. Jain, D. Neill, and I. Z. Rothstein, J. High Energy Phys. 05 (2012) 084.
[96] Y. Li, D. Neill, and H. X. Zhu, Nucl. Phys. **B960**, 115193 (2020).
[97] M. A. Ebert, I. Moult, I. W. Stewart, F. J. Tackmann, G. Vita, and H. X. Zhu, J. High Energy Phys. 04 (2019) 123.
[98] M. L. Miller, K. Reygers, S. J. Sanders, and P. Steinberg, Annu. Rev. Nucl. Part. Sci. **57**, 205 (2007).
[99] A. M. Sirunyan *et al.* (CMS Collaboration), Phys. Rev. Lett. **127**, 122001 (2021).
[100] ATLAS Collaboration, J. High Energy Phys. 06 (2023) 182.
[101] A. Gao, J. K. L. Michel, I. W. Stewart, and Z. Sun, Phys. Rev. D **107**, L091504 (2023).
[102] T. Liu, W. Melnitchouk, J.-W. Qiu, and N. Sato, Phys. Rev. D **104**, 094033 (2021).
[103] T. Liu, W. Melnitchouk, J.-W. Qiu, and N. Sato, J. High Energy Phys. 11 (2021) 157.